ARL-TR-8299 ● FEB 2018

US Army Research Laboratory

Assessment of the Tensile Properties for Single Fibers

by Julia Cline, Vincent Wu, and Paul Moy

NOTICES

Disclaimers

The findings in this report are not to be construed as an official Department of the Army position unless so designated by other authorized documents.

Citation of manufacturer's or trade names does not constitute an official endorsement or approval of the use thereof.

Destroy this report when it is no longer needed. Do not return it to the originator.

ARL-TR-8299 ● FEB 2018

US Army Research Laboratory

Assessment of the Tensile Properties for Single Fibers

by Julia Cline and Vincent Wu
Oak Ridge Institute for Science and Education, Oak Ridge, TN

Paul Moy
Weapons and Materials Research Directorate, ARL

REPORT DOCUMENTATION PAGE

Form Approved
OMB No. 0704-0188

1. REPORT DATE *(DD-MM-YYYY)*	2. REPORT TYPE	3. DATES COVERED (From - To)
February 2018	Technical Report	January–December 2017

4. TITLE AND SUBTITLE
Assessment of the Tensile Properties for Single Fibers

5a. CONTRACT NUMBER
1120-1120-99

5b. GRANT NUMBER

5c. PROGRAM ELEMENT NUMBER

6. AUTHOR(S)
Julia Cline, Vincent Wu, and Paul Moy

5d. PROJECT NUMBER
AH84

5e. TASK NUMBER

5f. WORK UNIT NUMBER

7. PERFORMING ORGANIZATION NAME(S) AND ADDRESS(ES)
US Army Research Laboratory
Weapons and Materials Research Directorate (ATTN: RDRL-WMM-B)
Aberdeen Proving Ground, MD 21005

8. PERFORMING ORGANIZATION REPORT NUMBER
ARL-TR-8299

9. SPONSORING/MONITORING AGENCY NAME(S) AND ADDRESS(ES)

10. SPONSOR/MONITOR'S ACRONYM(S)

11. SPONSOR/MONITOR'S REPORT NUMBER(S)

12. DISTRIBUTION/AVAILABILITY STATEMENT

13. SUPPLEMENTARY NOTES
Approved for public release; distribution is unlimited.

14. ABSTRACT

A novel experimental test method is presented to assess the tensile properties of single fibers, which pairs a Psylotech Nano-test system small-scale test frame with a Keyence 3-D laser scanning confocal microscope. This enables in situ optical microscopy to obtain fiber diameter measurements for each tensile experiment and thus improves the accuracy of calculated tensile properties. In this work, the developed test method is used to determine the tensile material properties for 4 types of Kevlar fiber. Results are presented and trends associated with fiber diameter are discussed.

15. SUBJECT TERMS
single fiber, mechanical characterization, Kevlar, tensile properties, in situ optical microscopy

16. SECURITY CLASSIFICATION OF:			17. LIMITATION OF ABSTRACT	18. NUMBER OF PAGES	19a. NAME OF RESPONSIBLE PERSON
a. REPORT	b. ABSTRACT	c. THIS PAGE			Julia Cline
Unclassified	Unclassified	Unclassified	UU	40	19b. TELEPHONE NUMBER (Include area code) 410-306-1949

Contents

List of Figures iv

List of Tables v

Acknowledgments vi

1. Introduction 1

2. Experimental Procedure 2

2.1 Test Equipment 2

2.2 Material 2

2.3 Single-Fiber Specimen Preparation 3

2.4 Installing the Specimen 5

2.5 Imaging Specimen 7

2.6 Test Method 9

2.7 Compliance Correction 9

3. Analysis 9

4. Results 11

5. Discussion 14

6. Property Variance with Respect to Diameter 18

7. Conclusions 24

8. References 25

Appendix. Kevlar Analysis Results 27

Distribution List 32

List of Figures

Fig. 1 Fiber specimen mounted on laser cut cardstock frame. a) Laser cut frames laid out in a grid pattern and multiple specimens drawn from a single fiber and b) zoomed-in view of a specimen. 4

Fig. 2 Mounting frame dimensions for a) 5-mm gage length sample and b) 15-mm gage length sample. All dimensions are given in millimeters. 5

Fig. 3 Fiber sample installed in the Psylotech nTS prior to the frame being cut..... 6

Fig. 4 The Psylotech nTS is placed under the Keyence microscope objective lens to enable in situ fiber diameter measurements 7

Fig. 5 The coordinate system defining the experimental setup with the x-direction along the length of the fiber and the direction of loading; the y-direction transverse to the fiber and the z-direction out of plane 8

Fig. 6 A laser confocal microscope image of a K29 single fiber at 100× magnification 9

Fig. 7 Example of K29 fiber diameter measurement using an image captured with the Keyence laser confocal microscope..... 10

Fig. 8 Tensile stress–strain curves for K119 single-fiber specimens. Specimens drawn from the same originating single fiber are grouped by color. 12

Fig. 9 Tensile stress–strain curves for K29 single-fiber specimens. Specimens drawn from the same originating single fiber are grouped by color… 12

Fig. 10 Tensile stress–strain curves for KM2+ single-fiber specimens. Specimens drawn from the same originating single fiber are grouped by color. 13

Fig. 11 Tensile stress–strain curves for K49 single-fiber specimens. Specimens drawn from the same originating single fiber are grouped by color… 13

Fig. 12 a) Tensile strength, b) tensile modulus, and c) strain to failure for single fibers as compared with published yarn data 15

Fig. 13 A comparison of the single fiber a) tensile strength, b) tensile modulus, and c) strain to failure for K119, K29, and K49 as measured in this work and by Naito..... 17

Fig. 14 Normalized values of tensile strength, strain to failure, and tensile modulus for Kevlar fibers 18

Fig. 15 Comparison of the tensile strength of K29 fibers calculated using assumed diameter and measured diameter values 19

Fig. 16 Stress–true strain curves for Kevlar K29 single-fiber specimens as calculated with an assumed fiber diameter of 12 μm 20

Fig. 17 The variation of a) tensile strength, b) tensile modulus, and c) strain to failure with fiber diameter for Kevlar fibers 21

List of Tables

Table 1 Properties of Kevlar aramid fiber yarns. 3

Table 2 Average values and standard deviation for each fiber type 14

Table 3 Average fiber diameter measurements for K29, K49, K119, and KM2+ single fibers 19

Table 4 Correlation of tensile strength to fiber diameter 23

Table 5 Correlation of tensile modulus to fiber diameter 23

Table 6 Correlation of strain to failure to fiber diameter 23

Table A-1 Analysis results for Kevlar K119 single-fiber tests (15-mm gage length) 28

Table A-2 Analysis results for Kevlar K119 single-fiber tests (5-mm gage length) 28

Table A-3 Analysis results for Kevlar K29 single-fiber tests (15-mm gage length) 29

Table A-4 Analysis results for Kevlar K29 single-fiber tests (5-mm gage length) 29

Table A-5 Analysis results for Kevlar KM2+ single-fiber tests (15-mm gage length) 30

Table A-6 Analysis results for Kevlar KM2+ single-fiber tests (5-mm gage length) 30

Table A-7 Analysis results for Kevlar K49 single-fiber tests (15-mm gage length) 31

Table A-8 Analysis results for Kevlar K49 single-fiber tests (5-mm gage length) 31

Acknowledgments

The authors acknowledge the technical conversations and helpful comments of Drs Kenneth Strawhecker and Michael Roenbeck of the US Army Research Laboratory (ARL) in conducting this study and in preparation of this technical report. This research was supported in part by an appointment to the Postgraduate Research Participation Program at ARL administered by the Oak Ridge Institute for Science and Education through an interagency agreement between the US Department of Energy and ARL.

1. Introduction

Fibers are the load-carrying constituent of fiber-reinforced composite materials. The desirable traits of a fiber include high stiffness, high strength, and low density. Understanding the tensile properties of single-fiber filaments enables improved understanding of yarn mechanics, which in turn improves understanding of lamina and laminate behavior and betters predictive performance capabilities. Ballistic performance predictions rely heavily on fiber material properties (i.e., modulus, ultimate tensile strength, strain to failure, and density).[1] Advancements in ballistic performance track with incremental increases in fiber stiffness and strength. Recent work directed at understanding processing effects on the mechanical behavior of fibers has established a connection between internal microstructure and fiber tensile behavior.[2]

Numerous studies have been performed to assess the tensile properties of single-fiber filaments, most based on the methods described in the ASTM D3822, Standard Test Method for Tensile Properties of Single Textile Fibers,[3] and C1557-03, Standard Test Method for Tensile Strength and Young's Modulus of Fibers.[4] The effect of gage length[5–8] and strain rate[6–10] have been evaluated for many classes of fibers. Gripping of certain varieties of single fibers proves to be a challenge, and improved methods to grip fibers have been studied. The direct gripping method developed by Sanborn et al.[10] is used in this work.

Because of the small size, accurately measuring the fiber diameter is not a trivial task. Several approaches have been reported in the literature. One is to assume the fiber diameter based on manufacturer-specified values with no direct measurements made in their experimental work.[7] It has been found, though, that the diameter of certain types of fibers do deviate from these assumed values and this can have significant effects on the calculation of the tensile properties of a single fiber. High-resolution scanning electron microscope (SEM) images were used by Lim et al.[11] to more accurately measure the diameter of A265 fibers. Measurements of fiber diameter from 15 samples were taken and averaged to obtain a fiber diameter to use in property calculations. These diameter measurements were taken near the end of a long fiber that was later used to produce specimens for testing. Because diameter measurements were not directly made on the specimens actually tested raises concerns regarding how representative the diameter measurements are, as variation along a single fiber can be significant, especially at large lengths. Naito[12] used both laser scanning microscope images and SEM to measure fiber diameters on a wide array of fibers including K29, K49, and K119, but it is not clear from his work if the fiber diameters were made on the same fibers that were tested or if his average fiber diameter is also calculated in a similar way to Lim et al.[11]

To improve the accuracy of the tensile property measurement, an experimental approach is presented to meticulously measure the diameter of each fiber specimen in the gage section directly prior to testing using a laser confocal microscope. As the single-fiber specimen is installed in the test frame and the test frame is then placed under the microscope prior to obtaining fiber diameter measurements, the specimen can be tested immediately after measurements are collected. This eliminates the opportunity for damage to the specimen encountered when transferring it from the microscope to a freestanding test frame.

2. Experimental Procedure

2.1 Test Equipment

A test method is developed based on a novel combination of a Psylotech Nano-test system (nTS) small-scale load frame and a Keyence 3-D laser scanning confocal microscope. The nTS, designed and developed by Psylotech, Inc. (Evanston, IL), features a 10-mm stroke actuator with a closed loop control of approximately 3-nm displacement resolution and a force capacity of up to 40 N. To allow in situ microscopy during single-fiber tensile experiments, the nTS was mounted in a Keyence VK-X200 digital laser scanning microscope, which enables a greater depth of field and larger field of view than the typical stereomicroscope. This combination enables detailed noncontact measurement of the fiber diameter. This setup also facilitates in situ deformation measurement and investigation into the deformation mechanics of single fibers.[13]

2.2 Material

Four varieties of off-the-shelf Kevlar fibers are chosen for tensile testing: Kevlar 29 (K29), Kevlar 49 (K49), Kevlar 119 (K119), and Kevlar KM2 Plus (KM2+). Kevlar is a para-aramid fiber developed by DuPont[14] that is frequently used for ballistic applications because of its high strength, stiffness, and light weight. Chemical composition of the 4 fiber varieties is the same; however, the processing varies. K119 and K29 fibers are not subject to any postprocessing heat treatment (i.e., additional heating or stretching after initial fiber spinning). KM2+ and K49 are heat treated to different levels, with K49 being the highest.

K29 is the original Kevlar fiber family developed for body and vehicle armor, cut resistant gloves, and reinforcement applications. K49 is a high modulus–low elongation fiber used primarily for cabling, sporting goods, and aerospace applications. K119 is designed for applications that require a fiber that is flexible

with high elongation and fatigue resistance. KM2+ is a high tenacity, high toughness, finer denier fiber well suited for body armor applications.[14] A summary of Kevlar yarn properties is given in Table 1.

Table 1 Properties of Kevlar aramid fiber yarns.[14–17]

Property	Kevlar K119	Kevlar K29	Kevlar KM2+	Kevlar K49
Denier	1500	1500	600	1140
Density (g/cm^3)	1.44	1.44	1.45	1.45
Diameter (μm)	12	12	12	12
Tenacity (gpd)	23.8	23	28.4	23.6
Tensile strength (GPa)	3.1	2.9	3.6	2.9
Tensile modulus (GPa)	55	70	84	135
Strain to failure (%)	4.4	3.6	3.8	2.8

2.3 Single-Fiber Specimen Preparation

Approximately 0.5–1.0 m of yarn is cut from a spool of bulk Kevlar yarns. Individual fibers are teased out of the yarn and, to mitigate any twist in the fiber caused during the extraction, each fiber is hung overnight to allow the fiber to untwist on its own. A small weight (<1 g) is taped to the free end of the fiber to keep the fiber taut and remove residual stresses. Single fibers are then mounted onto cardstock frames (Fig. 1).

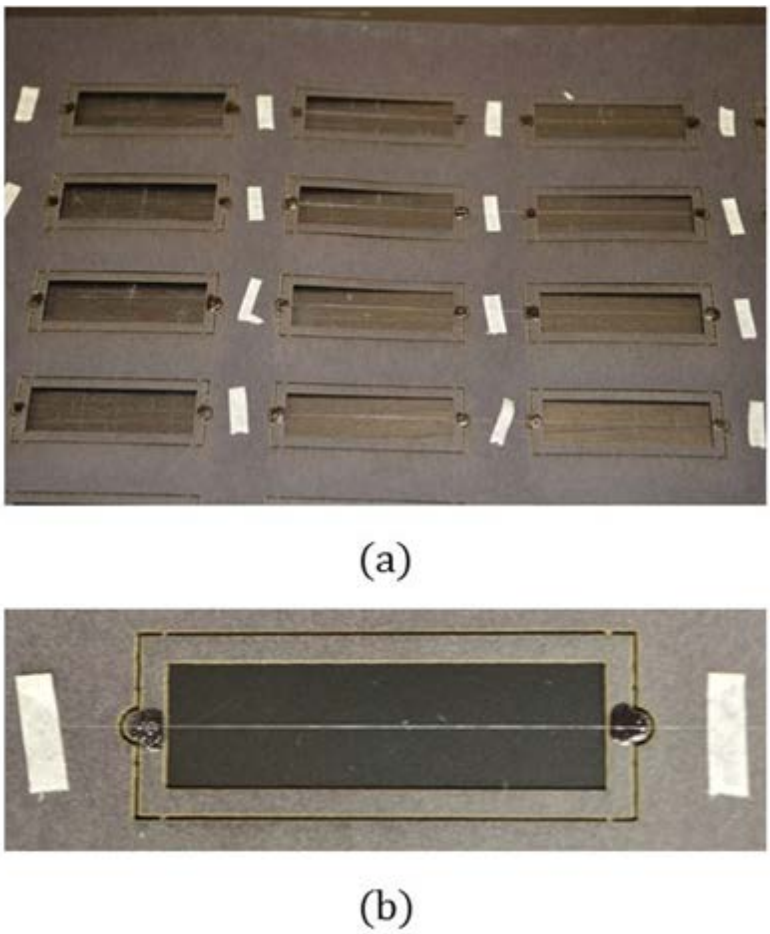

Fig. 1 Fiber specimen mounted on laser cut cardstock frame. a) Laser cut frames laid out in a grid pattern and multiple specimens drawn from a single fiber and b) zoomed-in view of a specimen.

The frame shape is cut from cardstock using a laser cutter in a grid formation. As shown in Fig. 1a, a single fiber is laid over several fiber mounts (i.e., multiple specimens can be drawn from a single fiber). Figure 1b shows a close-up of a single-fiber test specimen. The interior dimensions of the frame are designed to yield the desired fiber gage length. Specific dimensions for the frames used in this work are shown in Fig. 2 for gage lengths of 5 and 15 mm.

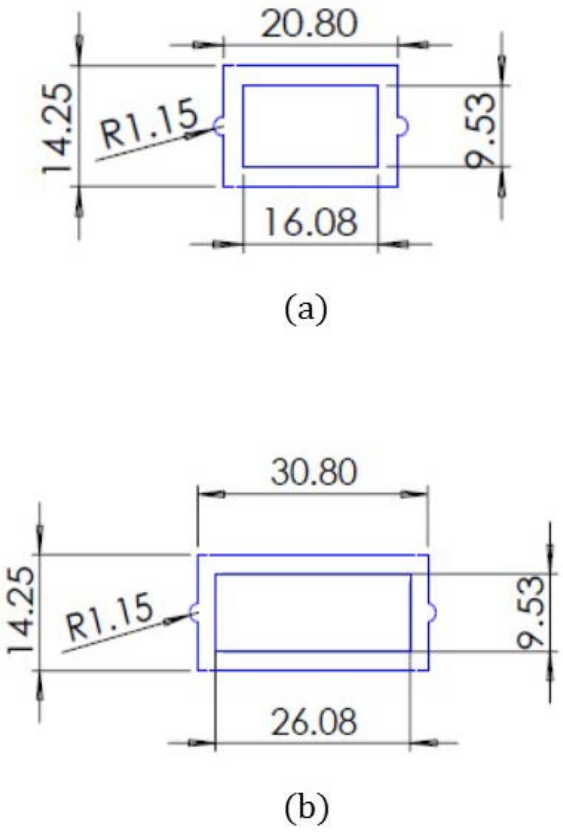

Fig. 2 Mounting frame dimensions for a) 5-mm gage length sample and b) 15-mm gage length sample. All dimensions are given in millimeters.

Adjustments are made to center the fiber on the mount by lining it up with horizontal alignment markers on the cardstock before it is temporarily secured into place using small strips of masking tape (Fig. 1b). Once the position is finalized, the fibers are secured into place using a small amount of cyanoacrylate (Gorilla Super Glue Impact Tough Formula) and left to dry overnight.

Approximately 20–25 specimens are prepared for each fiber type with a test gage length of 15 mm. To demonstrate that other gage lengths can be used with this experimental setup, 2–3 specimens from each fiber batch with a test gage length of 5 mm are also prepared. A full study on the effect of gage length on the tensile mechanical properties of single-fiber test specimens is beyond the scope of this work and will be completed in the future.

2.4 Installing the Specimen

The mounted specimen is cut out of the cardstock using an X-Actoknife and placed into the grips on the Psylotech nTS small-scale load frame as shown in Fig. 3. The frame mounts are designed with a hemispherical shape (Fig. 1b) at each end to

assist in the prealignment to the grip fixtures as well as adjust the actuator to the proper position. Using the tension-compression jog controls in the Psylotech software, the crosshead is moved to press the grips against the specimen as much as possible without deforming the cardstock frame. Practically, this can be observed as a change in the live load-displacement curve in the Psylotech software. Starting with the load cell side, the aluminum/polycarbonate tabs are applied to the specimen. All screws are finger-tightened first with the torx bit and then torqued to 0.44 in-lb using a torque driver. A direct gripping method is used,[10] where the fiber is sandwiched between 2 polycarbonate blocks.

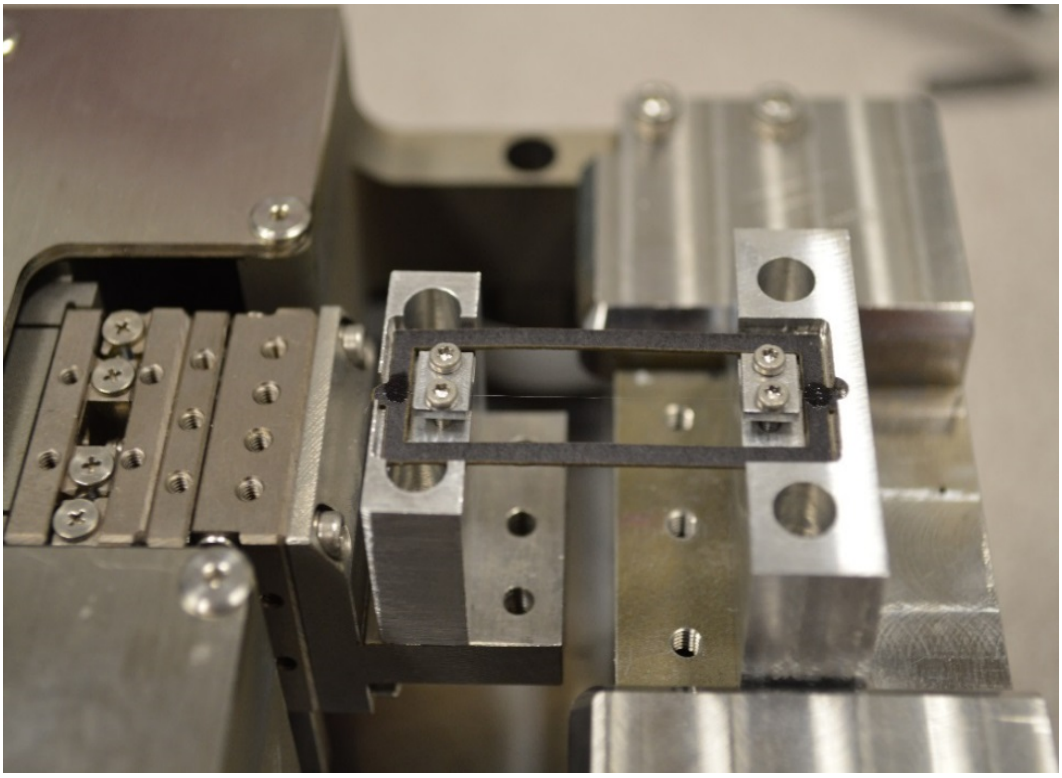

Fig. 3 Fiber sample installed in the Psylotech nTS prior to the frame being cut

Just prior to testing, the edges of the cardstock frame are cut. It is important that the edges do not touch each other during testing. Additionally, to promote the preservation of the tested sample for imaging after testing, it is important to ensure that the fiber remains attached to the cardboard mount. If a pair of tweezers is used to lightly hold the ends of the cardstock to prevent excessive twisting and bending during cutting, it is more likely the fiber will remain attached. The sides of the cardstock are snipped as close to the grips as possible.

Once the specimen is installed into the Psylotech, the Psylotech is placed under the microscope as shown in Fig. 4. Using the tension-compression jog feature set at a rate of 10 μm/s, the crosshead is moved until any pretension potentially applied

from the gripping process is removed (judged by when the live load-time curve plateaus). The "zero load" setting is turned on in the software indicating this is the approximate position of zero load on the sample. The tension jog is used to apply a preload to the sample. For this work, a preload between 500 and 1000 μN is used. Once the preload is set, the "zero displacement" setting is turned on in the software.

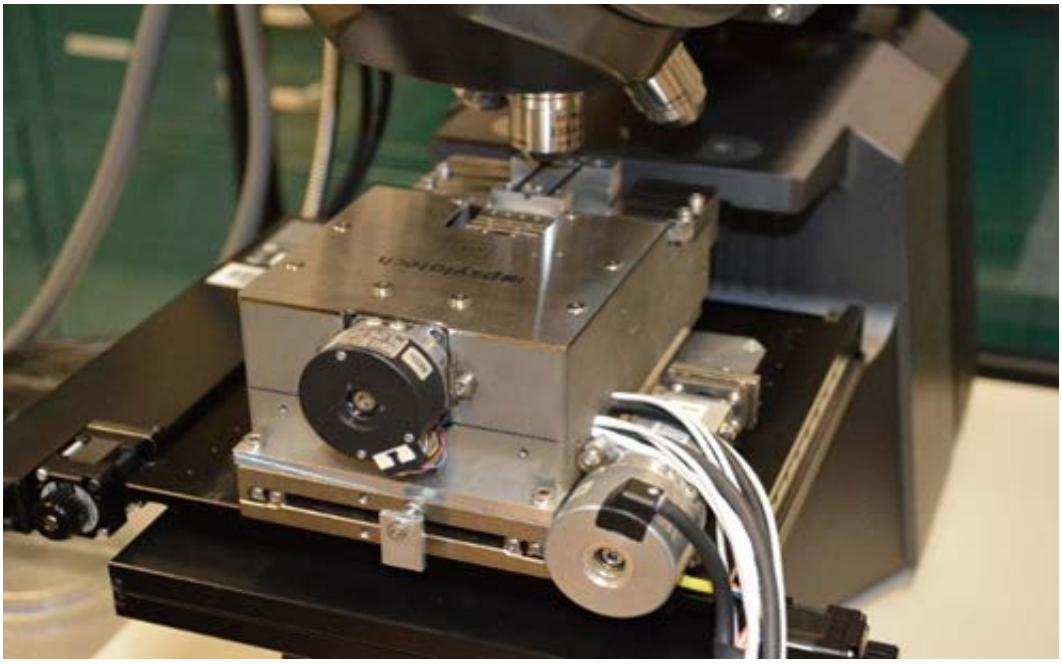

Fig. 4 The Psylotech nTS is placed under the Keyence microscope objective lens to enable in situ fiber diameter measurements

2.5 Imaging Specimen

For the process of acquiring single fiber diameter measurements, an image of a 450–500 μm section of the gage length is captured using the Keyence 3-D laser scanning confocal microscope prior to testing. The approximate middle of the gage length is focused first using the 5× objective lens, then under 10×, and finally 50× to assist in defining the field of view relative to the microscope stage position. Alignment of the fiber with the loading direction is important to ensure accurate results for the tensile properties of the fiber.[18] One unique feature of the Psylotech nTS is the ability to adjust the actuator in the y- and z-directions in 30-nm steps. For clarity, we define the directions as shown in Fig. 5. The x-direction is along the length of the fiber and is the direction of loading; the y-direction is transverse to the fiber, and the z-direction is out of plane. Adjusting the y-position allows precise alignment of the fiber with the loading direction (x-direction) and adjusting the z-position ensures that the entire length of the fiber is on the same focal plane.

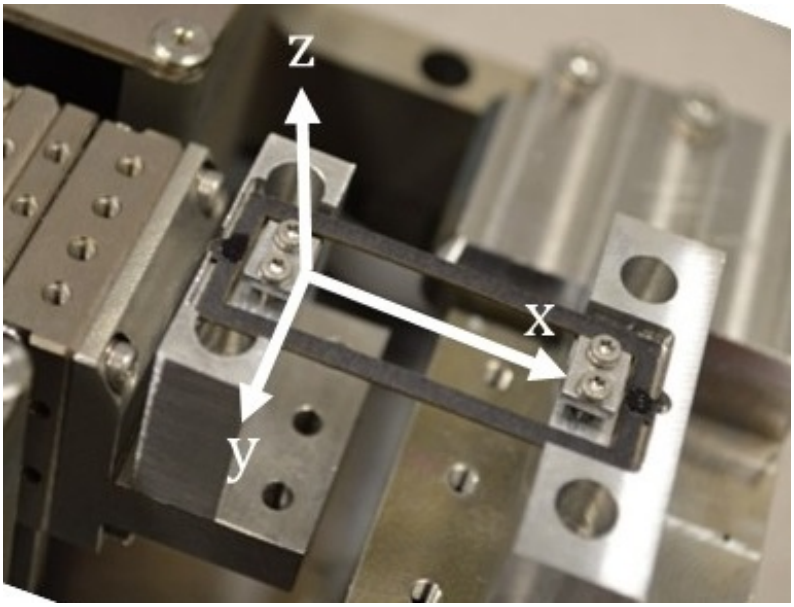

Fig. 5 The coordinate system defining the experimental setup with the x-direction along the length of the fiber and the direction of loading; the y-direction transverse to the fiber and the z-direction out of plane

Starting at the top of the gage length (load cell side), the fiber is centered and focused in the frame using the controls from the Keyence Viewer software. Any misalignment along the fiber gage length is noted. The actuator is adjusted by using the joystick to align (y-axis) and focus (z-axis) with respect to the fiber on the bottom of the gage length (actuator side). The alignment is again visually inspected between the top and bottom grip, and adjustments are made until the fiber is centered and focused along the entire gage length.

The final image of the fiber is taken using the 100× lens. The focus should be adjusted as necessary. Because the Keyence images in 3-D, we set the upper and lower bounds of the z-position of the lens turret to ensure that it captures the entire diameter of the fiber. In this work, the difference in the upper and lower bound was taken to be between 50 and 70 μm. The z-pitch is set to 0.20 μm, meaning that the 3-D slices will be taken at 0.20-μm intervals throughout the stretch between the designated upper and lower bounds. To capture an image of 450–500 μm of the gage section at 100×, 5 images must be captured and later stitched together. Once all settings are input, the Keyence starts the measurement to scan the fiber, which generally lasts 5–7 min. An example of one image of a K29 fiber is shown in Fig. 6.

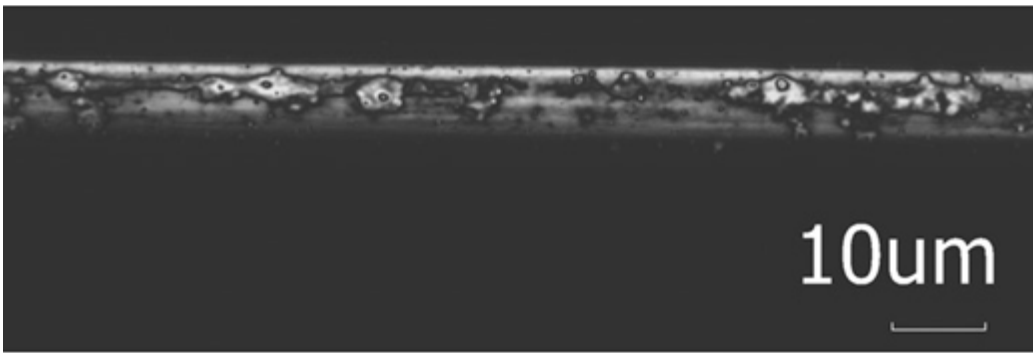

Fig. 6 A laser confocal microscope image of a K29 single fiber at 100× magnification

2.6 Test Method

The nTS is operated in displacement control mode at a rate of 4.5 μm/s for the 15-mm gage length samples and 1.5 μm/s for the 5-mm samples to ensure a quasi-static strain rate of $0.0003\ {}^{\varepsilon}/_{s}$. Load and crosshead displacement data are recorded by the Psylotech software. The test typically lasts between 2 and 4 min and stops manually several seconds after failure. Fiber fragments are recovered if possible and logged for posttest imaging and investigation of fracture surface.

2.7 Compliance Correction

The system compliance is measured in accordance with the procedure outlined in ASTM C1557.[4] Specimens are prepared with gage lengths of 15, 20, and 25 mm. Three tests are conducted for each gage length. The compliance correction factor that defines system compliance is calculated to be $C_s = 0.00009735$ m/N. This factor will be used during the analysis to remove any displacement associated with the system compliance from the total crosshead displacement.

3. Analysis

The 5 images, captured along the gage length of the fiber, are used to measure the diameter of the fiber via the Keyence VK Analysis software. The optical view mode, shown in Fig. 7, is found to give the best view of the entire fiber width. Using the 2-point tool, a line is drawn across the fiber width and the value is recorded. One diameter measurement is drawn from each image of the fiber gage sections.

The average of the 5 diameter measurements, d_{avg}, is used to calculate the cross-sectional area of the individual single fibers. The fibers are assumed to have a circular cross section.

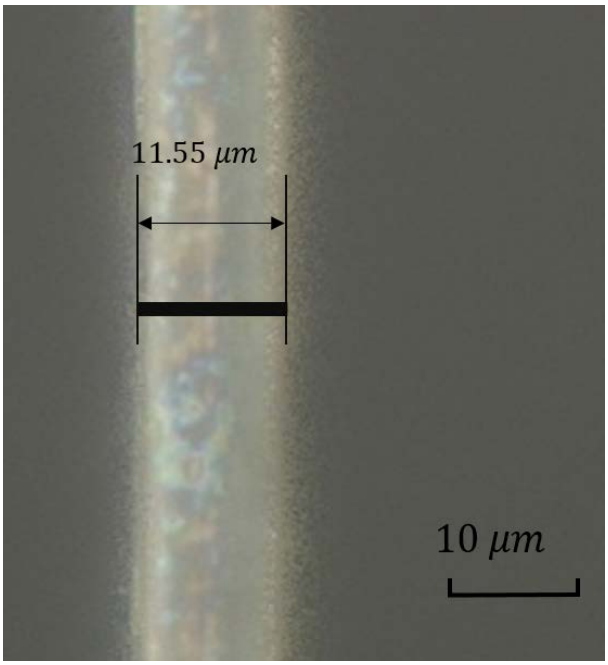

Fig. 7 Example of K29 fiber diameter measurement using an image captured with the Keyence laser confocal microscope

The time, crosshead displacement, and load data as recorded from the Psylotech are used to calculate stress, strain, and associated mechanical properties. Displacement and load data are corrected for the offset values at $t = 0$. The total crosshead displacement is also corrected for the effect of the system compliance. Engineering strain is calculated by dividing the corrected crosshead displacement, l, by the gage length, l_0.

$$\varepsilon = \frac{l}{l_0}. \tag{1}$$

Engineering stress is calculated as the applied load, P, divided by the undeformed cross-sectional area, A.

$$\sigma = \frac{P}{A}. \tag{2}$$

The ultimate tensile strength of the fiber, σ_{ult}, is defined as the maximum value of engineering stress. The tensile strain at σ_{ult} is also recorded as the strain to failure.

The tensile modulus is calculated as the slope of the line passing through 2 points on the stress–strain curve corresponding to tensile strain of $\varepsilon_{T,1} = 0.0001$ and $\varepsilon_{T,2} = 0.0010$ and their respective stress values.

$$E = \frac{\sigma(\varepsilon_2)-\sigma(\varepsilon_1)}{\varepsilon_2-\varepsilon_1}. \quad (3)$$

The strain rate for all tests is also calculated as the slope of the line passing through points on a strain versus time plot corresponding to $t_1 = 0\ s$ and $t_2 = 10\ s$.

$$\dot{\varepsilon} = \frac{\varepsilon(t_2)-\varepsilon(t_1)}{t_2-t_1}. \quad (4)$$

For all tests, the strain rate was calculated as $0.0003\ s^{-1}$, an appropriate value for an intended quasi-static test.

4. Results

Figures 8–11 show the stress–true strain plots for the 4 fiber types. To reiterate, for each of the 4 types of Kevlar tested, 4–6 long single fibers are extracted to produce 20–25 specimens per Kevlar fiber type. Samples prepared from the same single originating fiber are displayed with a unique color to distinguish them from samples produced from different originating single fibers. Interestingly, there is an even distribution of behavior for single-fiber specimens drawn from the same original fiber. The 5-mm gage length specimens are plotted alongside the 15-mm gage length specimens to directly compare the stress–strain response. The shorter gage length specimens exhibited a similar response to the longer gage length specimens, with some deviations noted for the K119 and K49 fibers. Only 2–3 specimens are tested for the shorter gage length, so more tests are necessary to truly comment on the effect of gage length on the experimental results. The specimens used to characterize the material response of the Kevlar fibers were of the longer gage length.

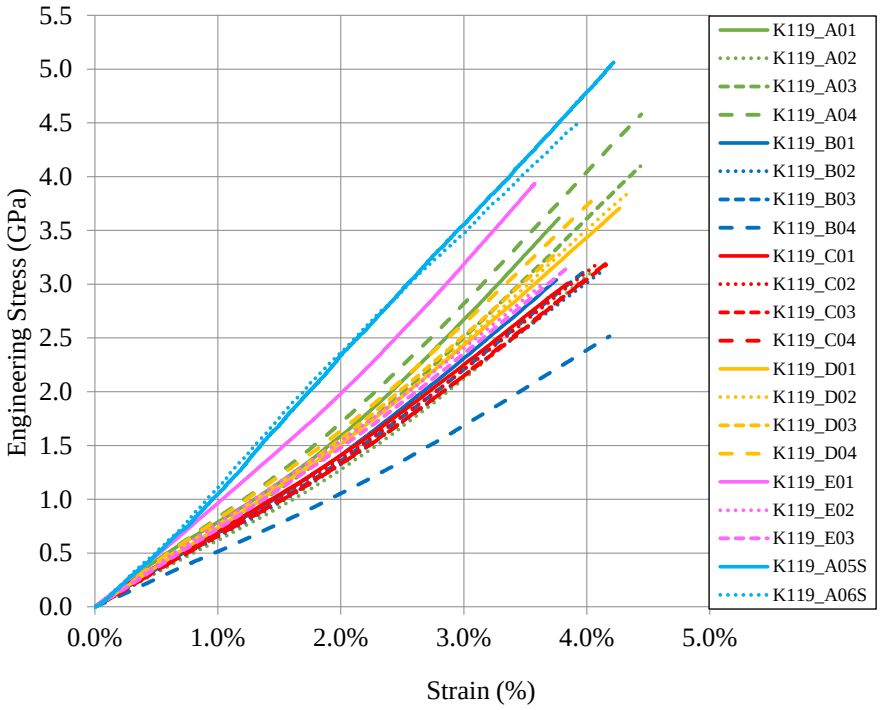

Fig. 8 Tensile stress–strain curves for K119 single-fiber specimens. Specimens drawn from the same originating single fiber are grouped by color.

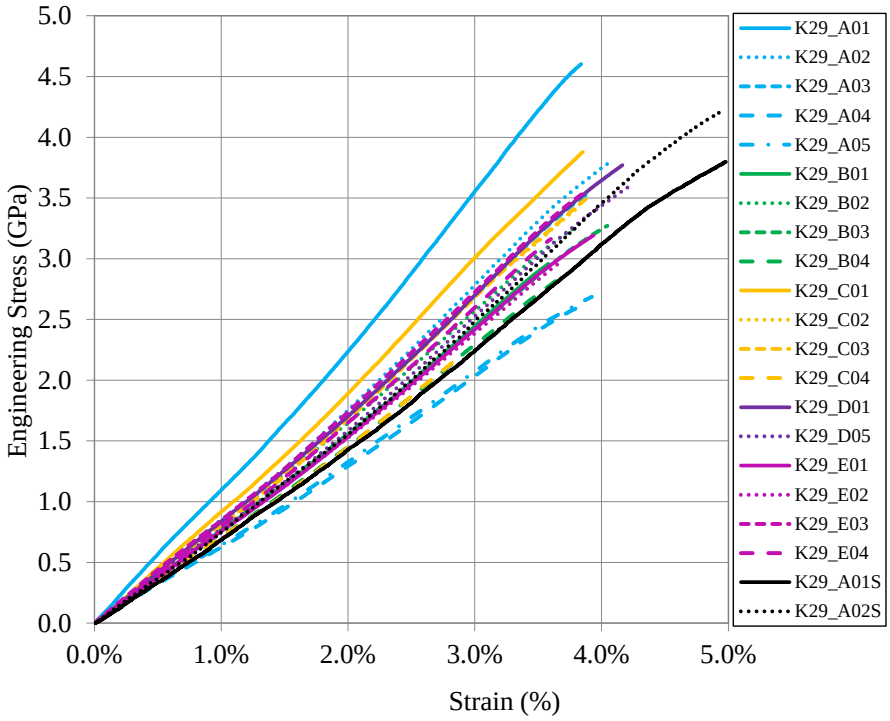

Fig. 9 Tensile stress–strain curves for K29 single-fiber specimens. Specimens drawn from the same originating single fiber are grouped by color.

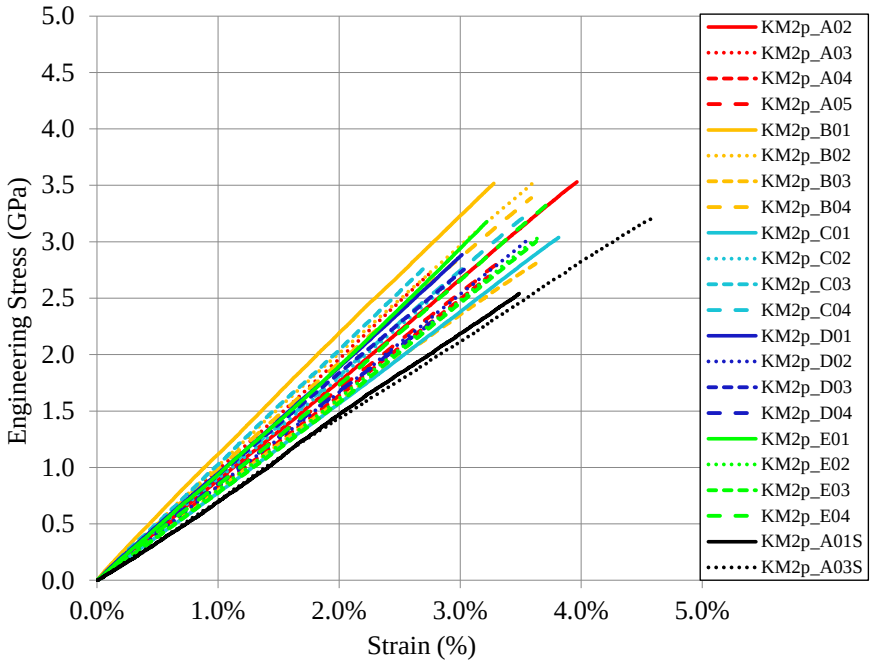

Fig. 10 Tensile stress–strain curves for KM2+ single-fiber specimens. Specimens drawn from the same originating single fiber are grouped by color.

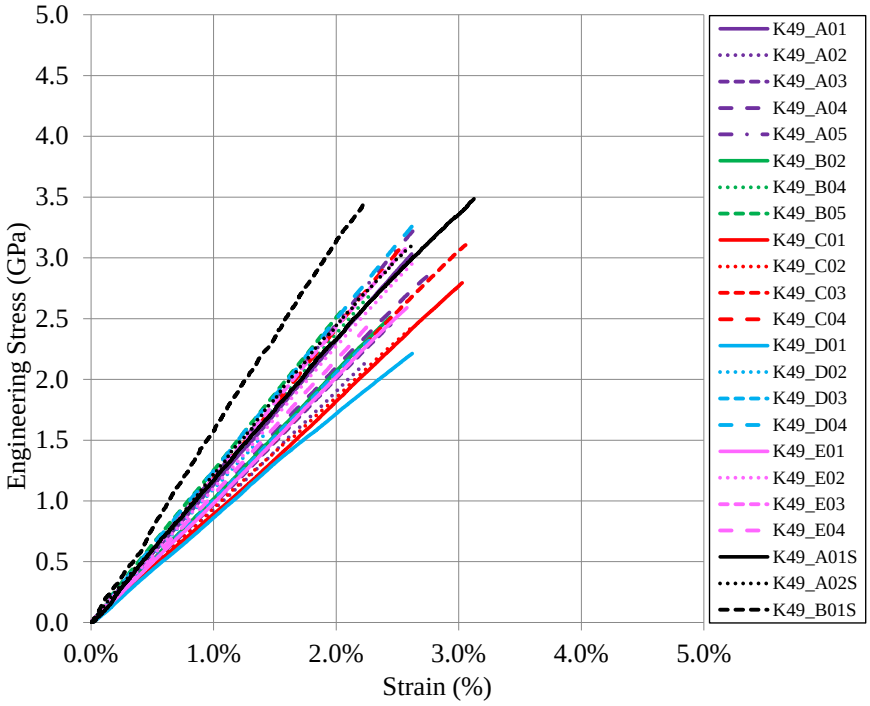

Fig. 11 Tensile stress–strain curves for K49 single-fiber specimens. Specimens drawn from the same originating single fiber are grouped by color.

5. Discussion

Some scatter is evident in the stress–strain curves (Figs. 8–11) for the single-fiber tension tests. Single-fiber tests are statistical in nature and depend on defects (or voids) within the fiber. The fiber tensile properties typically follow a Weibull distribution, which relates the distribution of strength, modulus, and strain to failure with flaw sensitivity.[12] Evaluating the Weibull modulus for these sets of Kevlar fibers is beyond the scope of this work.

Furthermore, shorter gage lengths tend to have larger scatter than longer gage lengths. The likelihood of a defect being present is higher for longer gage lengths, meaning that defects are likely to be present in each specimen tested. Rather, for shorter gage lengths, depending on the frequency of a defect along the length of a fiber, there could be specimens that are defect free and thus exhibit superior material properties to those specimens that contain a defect. In his work, Ou et al.[7] showed that increased gage lengths for K29 fibers reduced the scatter between individual specimens within a sample. The gage lengths used in this work are on the shorter end to what was used in Ou's work, so the expectation is that some scatter will exist in this data set.

Table 2 presents the numerical values for the average ultimate tensile strength, tensile modulus, and strain to failure for the fiber types. Full data tables for all specimens are included in the Appendix.

Table 2 Average values and standard deviation for each fiber type

Fiber system	Tensile strength (GPa)	Tensile modulus (GPa)	Strain to failure (%)
K119	3.4 ± 0.4	71.5 ± 7.7	4.0 ± 0.3
K29	3.3 ± 0.5	78.1 ± 9.6	3.8 ± 0.3
KM2+	3.0 ± 0.3	90.6 ± 11.6	3.4 ± 0.4
K49	2.7 ± 0.4	100.8 ± 12.9	2.5 ± 0.3

A comparison of the obtained fiber material properties (Table 2) and published yarn data[14–17] from Table 1 is shown in Fig. 12. The tensile modulus measurement for K49 single fibers differs the most with respect to yarn data. Otherwise, we see good agreement between single fiber and yarn data. The advantage of measuring the single fiber properties is that the values are independent of yarn mechanics.

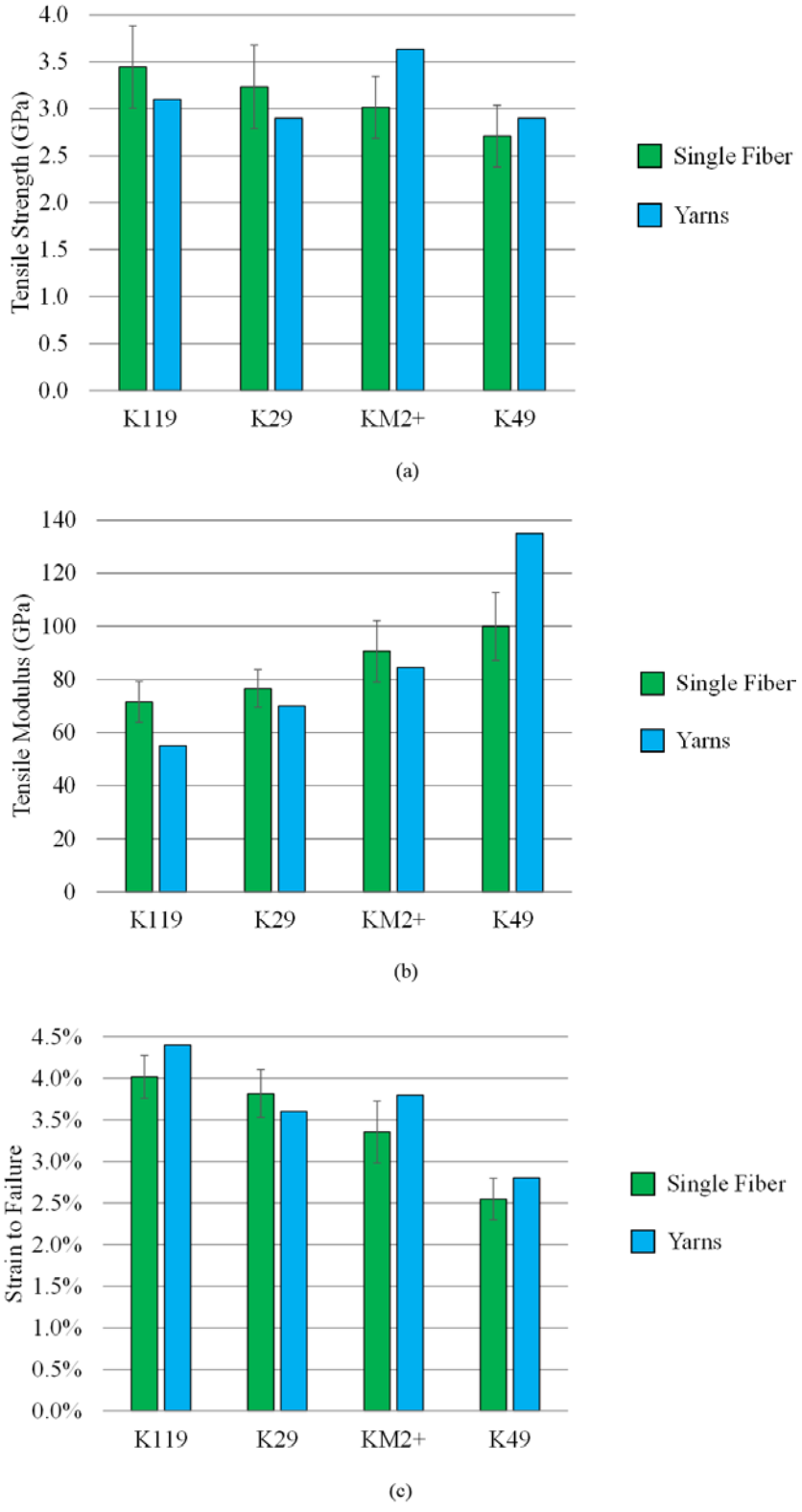

Fig. 12 a) Tensile strength, b) tensile modulus, and c) strain to failure for single fibers as compared with published yarn data[14–17]

Naito performed a comprehensive study of high-performance polymeric fibers including K29, K119, and K49 to understand their tensile properties.[12] His work included obtaining measurements of the fiber diameter using a laser scanning microscope and a high-resolution SEM but it is not clear from his work if he obtained fiber measurements on the specific fibers that were tested or from a representative sample drawn from similar yarns. A comparison of the average material properties obtained in this work (Table 2) with those of Naito is presented in Fig. 13, with the error bars indicating 1 standard deviation from the mean values. The variability in each material property calculated is on the same order between our data and Naito's, indicating that this is a true material variability, not necessarily method variability. The K119 and K29 fiber material properties obtained by our methods and by Naito are in good agreement (i.e., within the respective percent variations of the mean, which gives good confidence that these are truly the properties of the material). Some discrepancy is evident in the tensile modulus and strength for K49 fibers. This is potentially due to the difference in measured fiber diameter. Naito reports the average measured diameter of K49 fibers as 10.27 ± 0.78 μm, whereas our measurements indicate the average fiber diameter of our K49 fiber samples as 12.98 ± 0.57 μm. This 26% increase in diameter certainly does affect both calculated values for tensile strength and modulus. Repeating calculations for these properties using our data and an average diameter size of 10.27 μm does in fact yield a tensile modulus of 160.3 GPa and a tensile strength of 4.3 GPa, which are much more agreeable to the Naito data for K49 fibers.

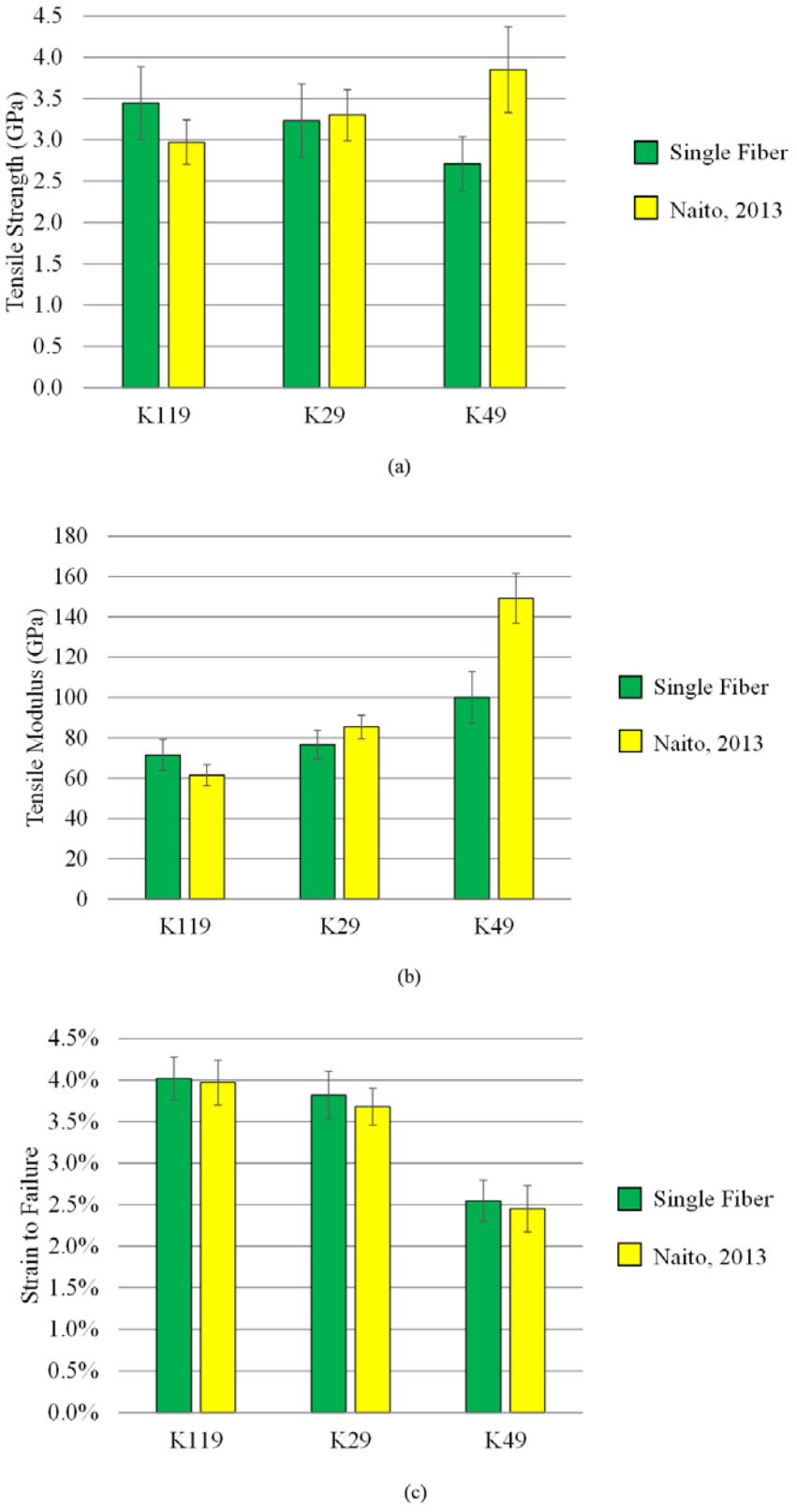

Fig. 13 A comparison of the single fiber a) tensile strength, b) tensile modulus, and c) strain to failure for K119, K29, and K49 as measured in this work and by Naito[12]

K29 is the original family of Kevlar products and thus considered to be the standard Kevlar[14] variety. Normalizing the average data to K29 allows for comparison among fiber types. Figure 14 plots the normalized average tensile strength, strain to failure, and tensile modulus for the Kevlar fibers. It is found that K49 fibers have the lowest tensile strength and strain to failure but the highest modulus. Conversely, K119 fibers have slightly higher strength and elongation than K29 fibers.

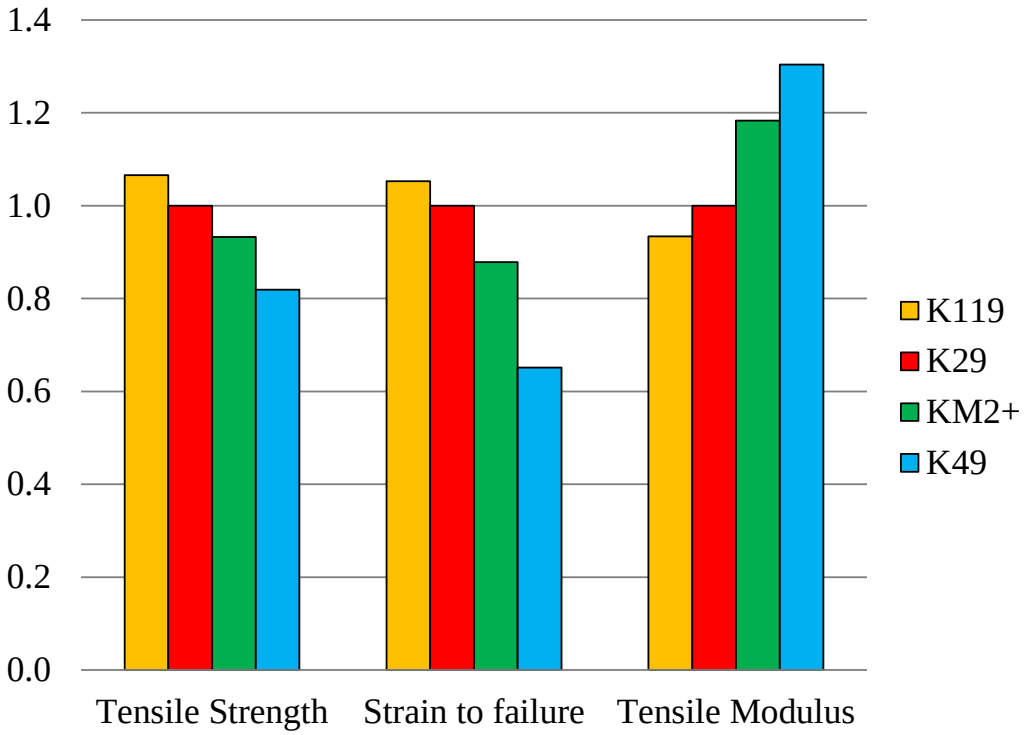

Fig. 14 Normalized values of tensile strength, strain to failure, and tensile modulus for Kevlar fibers

6. Property Variance with Respect to Diameter

In this work, great care is taken to accurately measure the fiber diameter, rather than relying on assumed fiber diameter measurements as specified by the manufacturer. Published data indicate a nominal fiber diameter of 12 μm for K29, K49, and K119, and 9–10 μm for KM2+[7,14]. However, the average values and standard deviations in fiber diameters, shown in Table 3, measured for our samples indicate that fiber diameter varies. This must be accounted for in stress calculations to yield accurate mechanical property calculations. The tabulated material properties presented thus far have been calculated based on actual fiber diameters.

Table 3 Average fiber diameter measurements for K29, K49, K119, and KM2+ single fibers

Fiber type	Fiber diameter (μm) ± 1 standard deviation
K119	12.42 μm ± 0.70 μm
K29	12.75 μm ± 0.78 μm
KM2+	11.18 μm ± 0.53 μm
K49	12.98 μm ± 0.57 μm

To demonstrate the importance of the fiber diameter in the analysis, the analysis of the K29 fibers is redone assuming a known diameter of 12 μm for each fiber. It can be observed from Fig. 15 that the tensile strength of the fibers calculated based on the assumed diameter of 12 μm is scattered. However, when the tensile strength is calculated based on measured diameter, a linear relationship between tensile strength and fiber diameter is discovered. In the case shown here, the importance of measuring the fiber diameter accurately can be understood by comparing the strengths of the specimens with the smallest and largest fiber diameters. The difference in strengths is on the order of several gigapascals, indicating just how significant of an effect the fiber diameter has on calculated material properties. Similar analysis can be repeated for the strain to failure and tensile modulus.

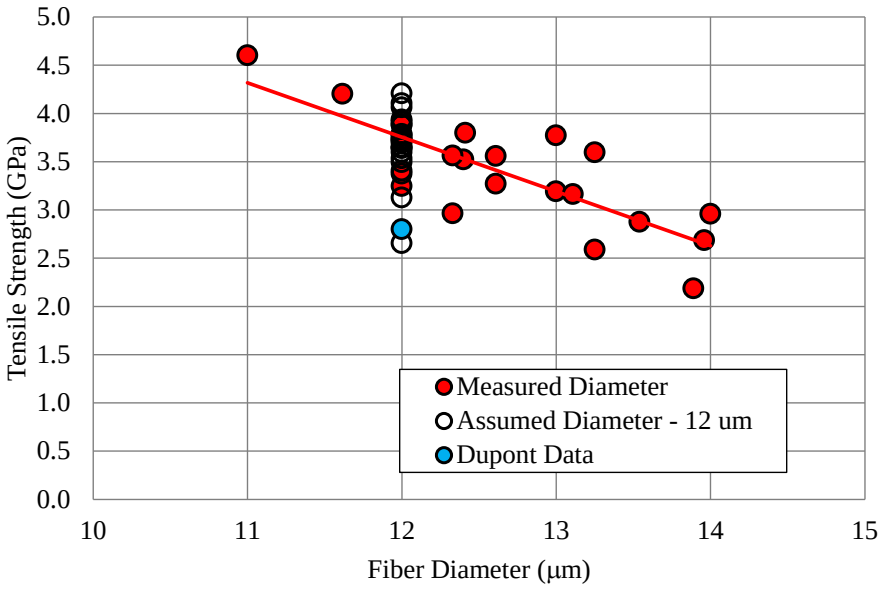

Fig. 15 Comparison of the tensile strength of K29 fibers calculated using assumed diameter and measured diameter values

To further illustrate the importance of measuring individual fiber diameters, we refer to Fig. 16. The raw data for the K29 single-fiber specimens that were used to generate Fig. 9 is reprocessed using an assumed diameter for each fiber of 12 μm.

For simplicity, we will refer to the analyses as Case 1 (measuring individual fiber diameters using the method developed in this report) and Case 2 (assuming a fiber diameter of 12 μm). Comparing the 2 figures, we see that the scatter in the stress–strain behavior for Case 2 is reduced compared with Case 1. Additionally, in Case 2, the 5-mm gage length samples seem to exhibit different behavior (reduced modulus, higher strength, higher strain to failure) than the 15-mm samples. In Case 1, the 5-mm samples fall within the scatter of the 15-mm samples. Clearly, the true scatter in single-fiber tensile data is not captured accurately if one follows the analysis method of Case 2. To obtain the most accurate stress calculation, it is imperative that the actual fiber diameter is measured for each individual single-fiber specimen.

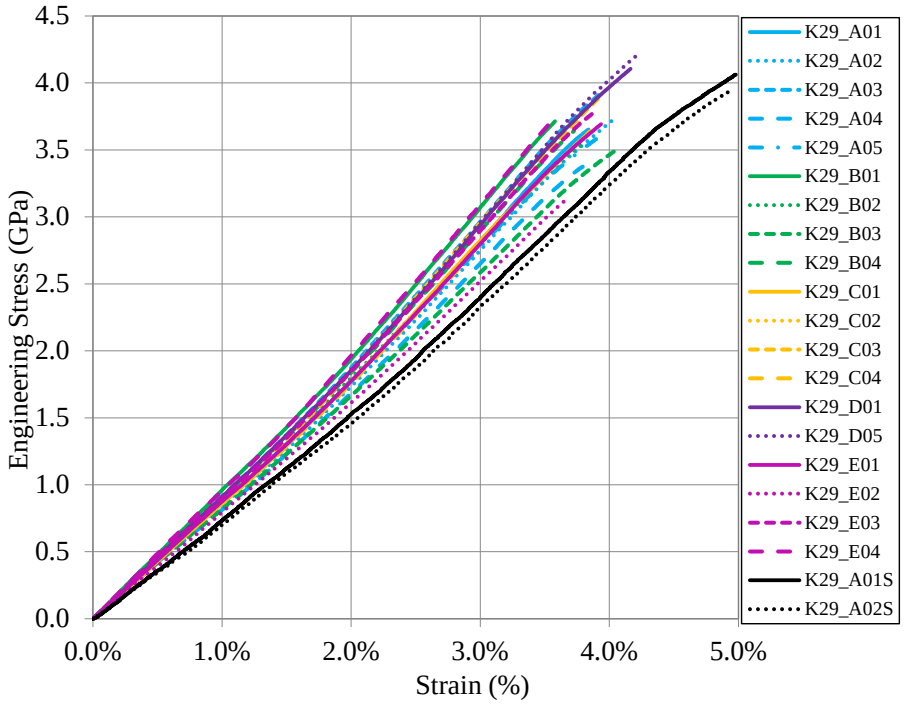

Fig. 16 Stress–true strain curves for Kevlar K29 single-fiber specimens as calculated with an assumed fiber diameter of 12 μm

The variation in fiber tensile strength with fiber diameter is plotted in Fig. 17a for all fiber systems. All Kevlar fiber varieties exhibit a linear decreasing relationship between tensile strength and fiber diameter. Likewise, similar plots are generated that compare the tensile modulus (Fig. 17b) and strain to failure (Fig. 17c) as a function of fiber diameter. In general, larger diameter fibers tend to have higher tensile strength and modulus, potentially indicating a higher degree of crystallite orientation as fiber diameter decreases.[19] A clear trend with fiber diameter is not evident for strain to failure for the Kevlar samples tested in this work.

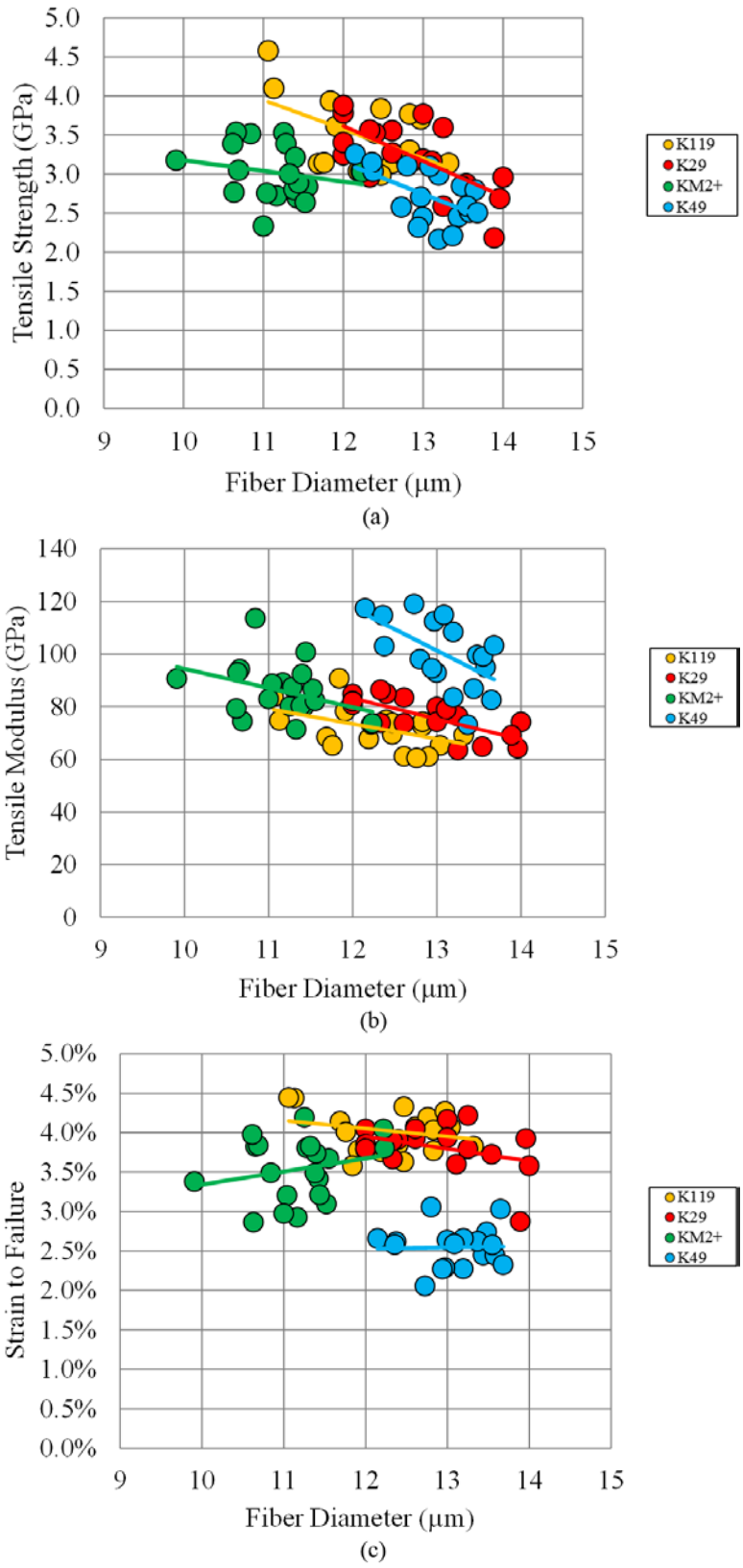

Fig. 17 The variation of a) tensile strength, b) tensile modulus, and c) strain to failure with fiber diameter for Kevlar fibers

To assess the linearity of the relationship between the material properties and the fiber diameter, we use Pearson's correlation coefficient,

$$r = \frac{\sum_{i=1}^{n}(x_i-\bar{x})(y_i-\bar{y})}{\sqrt{\sum_{i=1}^{n}(x_i-\bar{x})^2}\sqrt{\sum_{i=1}^{n}(y_i-\bar{y})^2}}, \quad (5)$$

where x_i and y_i are the sets of data points to be correlated, n is the number of data points, and $\bar{x}$, $\bar{y}$ are the mean values, that is

$$\bar{x} = \frac{1}{n}\sum^{n} x_i \quad (6)$$

and

$$\bar{x} = \frac{1}{n}\sum^{n} x_i \quad . \quad (7)$$

Conclusions can be drawn regarding the linearity of the relationship between the 2 quantities based on the sign and value of Pearson's correlation coefficient. Positive correlation ($0 < r < 1$) is defined as a direct relationship (both quantities increase or decrease with respect to one another). Negative correlation ($-1 < r < 0$) is defined as an inverse relationship (one quantity increases as the other decreases). A result of $r = 0$ indicates there is no linear relationship between the 2 quantities but does not negate any relationship all together. The absolute value of r indicates the strength of the correlation. The significance of the correlation is judged by a hypothesis test. We state the null and alternate hypothesis for a 2-tailed test:

H0: $r = 0$ (There is no linear relationship between x and y)

H1: $r \neq 0$ (There is a linear relationship between x and y)

Using Pearson's correlation coefficient, we look up the critical value of r, r_{crit}, in a table for the given number of degrees of freedom, $df = N - 2$, where N is the number of data pairs. We compare r to r_{crit} and if $|r| > r_{crit}$, we reject H0; otherwise, we retain H0.

A strong negative correlation is found between tensile strength and fiber diameter for K29 and K119 fibers, as shown in Fig. 17a. The null hypothesis is accepted for K49 and KM2+ fibers, indicating there is no linear relationship between fiber diameter and tensile strength. Details of the statistical analysis are shown in Table 4.

Table 4 Correlation of tensile strength to fiber diameter

Fiber type	Pearson's (r)	Number of samples (N)	Degrees of freedom (df)	Correlation (pos/neg)	Significance
K119	–0.637	19	17	Negative	$p<0.01$
K29	–0.782	19	17	Negative	$p<0.01$
KM2+	–0.223	20	18	Negative	Not significant
K49	–0.394	20	18	Negative	Not significant

All fiber types exhibit a significant, strong negative correlation between tensile modulus and fiber diameter with the exception of KM2+. From Fig. 17b, it is evident that K29 fibers exhibit the highest degree of linearity of tensile modulus with fiber diameter. Details of the statistical analysis are shown in Table 5.

Table 5 Correlation of tensile modulus to fiber diameter

Fiber type	Pearson's (r)	Number of samples (N)	Degrees of freedom (df)	Correlation (pos/neg)	Significance
K119	–0.607	19	17	Negative	$p<0.01$
K29	–0.823	19	17	Negative	$p<0.01$
KM2+	–0.339	20	18	Negative	Not significant
K49	–0.610	20	18	Negative	$p<0.01$

From Fig. 17, we can see that the strain to failure does not have a clear dependence on fiber diameter. Pearson's correlation coefficient analysis confirms that there is no significant linear relationship of strain to failure to fiber diameter. Details of the statistical analysis are shown in Table 6.

Table 6 Correlation of strain to failure to fiber diameter

Fiber type	Pearson's (r)	Number of samples (N)	Degrees of freedom (df)	Correlation (pos/neg)	Significance
K119	–0.147	19	17	Negative	Not significant
K29	–0.323	19	17	Negative	Not significant
KM2+	0.220	20	18	Positive	Not significant
K49	0.097	20	18	Positive	Not significant

7. Conclusions

A method for accurately characterizing the tensile material properties of single fibers incorporating in situ diameter measurements using a laser confocal microscope and a Psylotech nTS is presented in this work. Microscope images were used to extract diameter measurements for each specimen tested and averaged for use in calculations for engineering stress. Strain was calculated from the compliance-corrected crosshead displacement and the gage length of the specimen. The tensile strength, modulus, and strain to failure were calculated for each specimen tested, and the averages of the sample were reported as the tensile material properties for each fiber type. It has been demonstrated that using in situ microscopy for diameter measurements improves the accuracy of stress calculations for single fibers and, as such, the calculation of the tensile material properties. The data collected in this work showed good agreement with data from published works focused on single-fiber tensile properties.

Individually measuring the fiber diameter for each fiber specimen tested allowed us to identify trends in material properties with increasing fiber diameter. We found that there was up to a 6% variation in fiber diameter between the sets of specimens tested and that the fiber diameter varied along the length of a single fiber. This indicates the importance of carefully measuring fiber diameters for each specimen, rather than just a representative sample or using an averaged value. Statistical analysis showed that a linear decreasing relationship between fiber diameter and tensile strength exists for K119 and K29 fibers and a linear decreasing relationship between fiber diameter and tensile modulus for K119, K29, and K49 fibers. Variability in the measurements is attributed to the variability of the material.

8. References

1. Cunniff PM. Dimensionless parameters for optimization of textile-based body armor systems. Proceedings of the 18th International Symposium On Ballistics; 1999; San Antonio, TX.

2. Roenbeck MR, Sandoz-Rosado EJ, Cline J, Wu V, Moy P, Afshari M, Reichert D, Lustig SR, Strawhecker KE. Probing the internal structures of Kevlar® fibers and their impacts on mechanical performance. Polymer. 2017;128:200–210.

3. ASTM D3822. Standard test method for tensile properties of single textile fibers. West Conshohocken (PA): ASTM International; 2014.

4. ASTM C1557-03. Standard test method for tensile strength and Young's modulus of fibers. West Conshohocken (PA): ASTM International; 2008.

5. Pardini LC, Manhani LGB. Influence of the testing gage length on the strength, Young's modulus and Weibull modulus of carbon fibres and glass fibres. Mat Res. 2002;5(4):411–420.

6. Lim J, Zheng J, Masters K, Chen W. Effects of gage length, loading rates and damage on the strength of PPTA fibers. Int J Imp Eng. 2011;38:219–227.

7. Ou Y, Zhu D, Huang M, Li H. The effects of gage length and strain rate on tensile behavior of Kevlar 29 single filament and yarn. J Comp Mat. 2017;51(1);109–123.

8. Lim J, Chen W. Dynamic small strain measurements of Kevlar 129 single fibers with a miniaturized tension Kolsky bar. Polym Test. 2010;29(6);701–705.

9. Wang Y, Xia Y. The effects of strain rate on the mechanical behavior of Kevlar fibre bundles: an experimental and theoretical study. Composites Part A. 1998;29A:1411–1415.

10. Sanborn B, DiLeonardi AM, Weerasooriya T. Tensile properties of Dyneema SK76 single fibers at multiple loading rates using a direct gripping method. Aberdeen Proving Ground (MD): Army Research Laboratory (US); 2014 June. Report No.: ARL-TR-6974.

11. Lim J, Zheng J, Masters K, Chen W. Mechanical behavior of A265 single fibers. J Mat Sci. 2010;45:652–662.

12. Naito K. Tensile properties and Weibull modulus of some high-performance polymeric fibers. J App Polym Sci. 2013;128(2):1185–1192.

13. Wu V, Moy P, Weerasooriya T. In-situ microscopy for displacement and strain measurements of UHMWPE single fibers in tension. Paper presented at: Society for the Advancement of Material and Process Engineering conference; 2016 May 23–26; Long Beach, CA.

14. DuPont. Technical guide: Kevlar Aramid fiber. Richmond (VA): DuPont Advanced Fiber Systems; no date [accessed 2018 Feb 6]. http://www.dupont.com/content/dam/dupont/products-and-services/fabrics-fibers-and-nonwovens/fibers/documents/DPT_Kevlar_Technical_Guide_Revised.pdf.

15. Ahmed D, Hongpeng Z, Haijuan K, Jing L, Yu M, Muhuo Y. Microstructural developments of poly (p-phenylene terephthalamide) fibers during heat treatment process: a review. Mat Res. 2014;17(5):1180–1200.

16. Dupont. Technical information: properties and processing of Dupont Kevlar® brand yarn for mechanical rubber goods. Richmond (VA): DuPont Advanced Fiber Systems; no date [accessed 2018 Jan 10]. http://www.dupont.co.uk/content/dam/dupont/products-and-services/fabrics-fibers-and-nonwovens/fibers/documents/Technical%20Guide%20for%20Kevlar%C2%AE%20in%20Mechanical%20Rubber%20Goods.pdf.

17. Cavallaro PV. Effects of weave styles and crimp gradients in woven Kevlar/epoxy composites. Exp Mech. 2016;56:617–635.

18. Wu V, Moy P. Influence of off-axis tensile loading on single fibers properties. Paper presented at: Society for the Advancement of Material and Process Engineering Conference; 2017 May 22–25; Seattle, WA.

19. Riekel C, Dieing T, Engström P, Vincze L, Martin C, Mahendrasingam A. X-ray microdiffraction study of chain orientation in poly (*p*-phenylene terephthalamide). Macromolecules. 1999;32:7859–7865.

Appendix. Kevlar Analysis Results

Table A-1 Analysis results for Kevlar K119 single-fiber tests (15-mm gage length)

Specimen	Diameter (μm)	Tensile strength (GPa)	Tensile modulus (GPa)	Strain to failure (%)
K119_A01	11.91	3.6	78.29	3.8
K119_A02	12.61	3.1	61.21	4.1
K119_A03	11.13	4.1	74.84	4.4
K119_A04	11.06	4.6	83.79	4.4
K119_B01	12.19	3.0	67.80	3.8
K119_B02	11.69	3.1	68.51	4.1
K119_B03	11.76	3.1	65.28	4.0
K119_B04	13.82	2.5	49.84	4.2
K119_C01	12.4	3.0	75.06	3.8
K119_C02	13.04	3.2	65.27	4.1
K119_C03	12.90	3.2	61.08	4.2
K119_C04	12.76	3.2	60.55	4.2
K119_D01	12.97	3.7	74.85	4.3
K119_D02	12.47	3.8	69.46	4.3
K119_D03	12.83	3.3	72.70	3.8
K119_D04	12.83	3.8	74.35	4.0
K119_E01	11.84	3.9	90.85	3.6
K119_E02	12.47	3.0	73.98	3.6
K119_E03	13.32	3.1	69.25	3.8
Average	12.42	3.4	70.36	4.0
Standard deviation	0.70	0.5	8.92	0.3

Table A-2 Analysis results for Kevlar K119 single-fiber tests (5-mm gage length)

Specimen	Diameter (μm)	Tensile strength (GPa)	Tensile modulus (GPa)	Strain to failure (%)
K119_A05S	10.10	5.1	80.15	4.2
K119_A06S	10.50	4.5	94.68	3.9

Table A-3 Analysis results for Kevlar K29 single-fiber tests (15-mm gage length)

Specimen	Diameter (μm)	Tensile strength (GPa)	Tensile modulus (GPa)	Strain to failure (%)
K29_A01	11.00	4.6	106.16	3.8
K29_A02	12.00	3.8	84.84	4.0
K29_A03	12.61	3.6	83.49	3.9
K29_A04	13.25	2.6	63.62	3.8
K29_A05	13.96	2.7	64.24	3.9
K29_B01	14.00	3.0	74.17	3.6
K29_B02	12.00	3.2	80.79	3.8
K29_B03	12.61	3.3	73.75	4.0
K29_B04	13.54	2.9	64.89	3.7
K29_C01	12.00	3.9	82.17	3.9
K29_C02	12.00	3.4	82.10	3.8
K29_C03	12.40	3.5	85.04	3.9
K29_C04	13.89	2.2	69.23	2.9
K29_D01	13.00	3.8	80.01	4.2
K29_D05	13.25	3.6	76.48	4.2
K29_E01	13.00	3.2	74.35	3.9
K29_E02	12.33	3.0	73.83	3.7
K29_E03	12.33	3.6	86.44	3.9
K29_E04	13.11	3.2	79.04	3.6
Average	12.75	3.3	78.14	3.8
Standard deviation	0.78	0.5	9.59	0.3

Table A-4 Analysis results for Kevlar K29 single-fiber tests (5-mm gage length)

Specimen	Diameter (μm)	Tensile strength (GPa)	Tensile modulus (GPa)	Strain to failure (%)
K29_A01S	12.41	3.8	61.22	5.0
K29_A02S	11.62	4.2	72.06	4.9

Table A-5 Analysis results for Kevlar KM2+ single-fiber tests (15-mm gage length)

Specimen	Diameter (μm)	Tensile strength (GPa)	Tensile modulus (GPa)	Strain to failure (%)
KM2p_A02	11.25	3.5	84.61	4.0
KM2p_A03	11.17	2.7	94.14	2.8
KM2p_A04	11.42	2.7	84.95	3.2
KM2p_A05	11.38	2.8	85.71	3.3
KM2p_B01	10.84	3.5	123.91	3.3
KM2p_B02	10.66	3.5	98.75	3.6
KM2p_B03	11.55	2.8	82.24	3.7
KM2p_B04	11.28	3.4	94.93	3.6
KM2p_C01	12.22	3.0	77.69	3.8
KM2p_C02	11.52	2.6	91.73	2.9
KM2p_C03	10.63	2.8	98.47	2.7
KM2p_C04	11.40	3.2	98.15	3.5
KM2p_D01	11.44	2.9	107.26	3.0
KM2p_D02	12.23	3.0	79.68	3.6
KM2p_D03	11.04	2.8	94.27	3.0
KM2p_D04	11.00	2.3	87.42	2.8
KM2p_E01	9.91	3.2	95.65	3.2
KM2p_E02	10.69	3.0	76.11	3.7
KM2p_E03	11.33	3.0	72.99	3.6
KM2p_E04	10.62	3.4	83.32	3.8
Average	11.18	3.0	90.60	3.4
Standard deviation	0.53	0.3	11.56	0.4

Table A-6 Analysis results for Kevlar KM2+ single-fiber tests (5-mm gage length)

Specimen	Diameter (μm)	Tensile strength (GPa)	Tensile modulus (GPa)	Strain to failure (%)
KM2p_A01S	11.87	2.5	63.23	3.5
KM2p_A03S	11.71	3.2	65.40	4.6

Table A-7 Analysis results for Kevlar K49 single-fiber tests (15-mm gage length)

Specimen	Diameter (μm)	Tensile strength (GPa)	Tensile modulus (GPa)	Strain to failure (%)
K49_A01	12.37	3.0	103.07	2.6
K49_A02	13.19	2.2	83.58	2.3
K49_A03	13.44	2.5	86.91	2.4
K49_A04	13.48	2.8	99.76	2.7
K49_A05	12.15	3.3	117.45	2.7
K49_B02	13.58	2.5	95.02	2.4
K49_B04	12.97	2.7	112.50	2.3
K49_B05	12.73	2.6	119.10	2.1
K49_C01	13.65	2.8	82.64	3.0
K49_C02	13.00	2.4	92.92	2.6
K49_C03	12.80	3.1	98.13	3.1
K49_C04	12.36	3.1	114.81	2.6
K49_D01	13.37	2.2	73.10	2.6
K49_D02	12.60	1.5	97.60	1.4
K49_D03	12.94	2.3	94.64	2.3
K49_D04	11.44	3.3	119.46	2.6
K49_E01	13.55	2.6	99.09	2.6
K49_E02	13.20	3.0	108.48	2.7
K49_E03	13.08	3.1	114.97	2.6
K49_E04	13.68	2.5	103.29	2.3
Average	12.98	2.7	100.8	2.5
Standard deviation	0.57	0.4	12.9	0.3

Table A-8 Analysis results for Kevlar K49 single-fiber tests (5-mm gage length)

Specimen	Diameter (μm)	Tensile strength (GPa)	Tensile modulus (GPa)	Strain to failure (%)
K49_A01S	12.88	3.5	93.64	3.1
K49_A02S	13.23	3.1	127.92	2.6
K49_B01S	10.83	3.5	185.51	2.2

1 (PDF) DEFENSE TECHNICAL INFORMATION CTR
DTIC OCA

2 (PDF) DIR ARL
IMAL HRA
RECORDS MGMT
RDRL DCL
TECH LIB

1 (PDF) GOVT PRINTG OFC
A MALHOTRA

35 (PDF) DIR ARL
RDRL WMM A
E WETZEL
E SANDOZ-ROSADO
M ROENBECK
K STRAWHECKER
T BOGETTI
J STANISZEWSKI
B PATTERSON
M PLOCH
J SANDS
T PLAISTED
J TZENG
C YEN
D O'BRIEN
M WALTER
D SPAGNUOLO
K SHANNON
D KNORR
RDRL WMM B
J CLINE
V WU
P MOY
B LOVE
T WALTER
B POWERS
RDRL WMM G
J LENHART
K MASSER
R MROZEK
J PARK
J ANDZELM
J YU
RDRL WMP B
T WEERASOORIYA
A GUNNARSSON
C HOPPEL
T ZHANG
J MCKEE
RDRL WMP C
S SATAPATHY